

DSCD-Nav: Dual-Stance Cooperative Debate for Object Navigation

Weitao An¹ Qi Liu¹ Chenghao Xu² Jiayi Chai¹ Xu Yang¹ Kun Wei¹ Cheng Deng¹

Abstract

Adaptive navigation in unfamiliar indoor environments is crucial for household service robots. Despite advances in zero-shot perception and reasoning from vision-language models, existing navigation systems still rely on single-pass scoring at the decision layer, leading to overconfident long-horizon errors and redundant exploration. To tackle these problems, we propose Dual-Stance Cooperative Debate Navigation (DSCD-Nav), a decision mechanism that replaces one-shot scoring with stance-based cross-checking and evidence-aware arbitration to improve action reliability under partial observability. Specifically, given the same observation and candidate action set, we explicitly construct two stances by conditioning the evaluation on diverse and complementary objectives: a Task-Scene Understanding (TSU) stance that prioritizes goal progress from scene-layout cues, and a Safety-Information Balancing (SIB) stance that emphasizes risk and information value. The stances conduct a cooperative debate and make policy by cross-checking their top candidates with cue-grounded arguments. Then, a Navigation Consensus Arbitration (NCA) agent is employed to consolidate both sides' reasons and evidence, optionally triggering lightweight micro-probing to verify uncertain choices, preserving NCA's primary intent while disambiguating. Experiments on HM3Dv1, HM3Dv2, and MP3D demonstrate consistent improvements in success and path efficiency while reducing exploration redundancy.

1. Introduction

Indoor service robots rely on robust navigation to reach target locations and support object-centric tasks. In zero-shot

¹School of Electronic Engineering, Xidian University, Xi'an 710071, China. ²School of Information Science and Engineering, Hohai University, Nanjing 210098, China. Correspondence to: Xu Yang <xuyang.xd@gmail.com>.

Preprint. February 3, 2026.

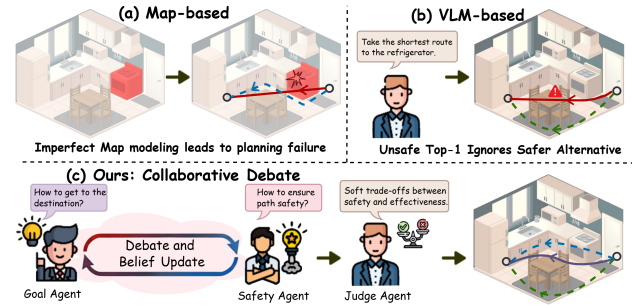


Figure 1. (a) Map-based navigation is brittle to map errors. (b) VLM-based navigation is overly confident, making greedy Top-1 choices. (c) Our DSCD-Nav uses collaborative debate and arbitration for more reliable decisions.

object navigation, an embodied agent must move from a random start to a target object in an unseen scene using only egocentric observations, without prior maps or task-specific training (Batra et al., 2020). With only partial views and an object-level goal (e.g., a category or short text query), the agent must interpret observations, explore for informative viewpoints, and make long-horizon decisions under incomplete evidence. This setting calls for a robust execution strategy for goal-directed, long-horizon movement.

Existing indoor navigation systems typically evolve from explicit mapping-and-planning pipelines to foundation-model-driven decision makers. Early approaches build structured spatial representations, including globally consistent topological graphs, semantic maps, or online occupancy grids, to support downstream planning and control (Busch et al., 2025; Jiang et al., 2025; Zhang et al., 2025a; Yin et al., 2024). When geometry and semantics are reliable, these map-centric pipelines can select waypoints efficiently and generate stable executable paths. More recently, to reduce reliance on precise maps and large-scale task training, LLMs and VLMs have been incorporated into navigation systems to enhance scene understanding and goal grounding (Wu et al., 2025; Goetting et al., 2024; Long et al., 2024). For example, an LLM can translate a goal or instruction into semantic sub-goals, while a VLM can directly score candidate directions or views from the current observation, enabling strong zero-shot behaviors (Nasiriany et al., 2024; Rajabi & Kosecka, 2025).

Despite their effectiveness, both paradigms remain brittle in complex indoor scenes, as action selection often commits to a single stream, slow to challenge or revise under partial evidence. In map-centric pipelines, occlusions, lighting variation, or clutter may introduce systematic errors into the constructed representation, yet the planner may still trust it and execute numerous steps before reacting (Raychaudhuri & Chang, 2025). As illustrated in Fig. 1(a), such over-commitment can trigger prolonged detours (*e.g.*, mistaking a corridor for a dead end) or repeated collisions from misjudging clutter as traversable. LLM/VLM-based agents reduce explicit mapping, but many still make one-shot decisions by scoring candidates once and executing the top-ranked action (Gu et al., 2025; Nie et al., 2025) as shown in Fig. 1(b). In both cases, goal progress, safety, and uncertainty are often compressed into a single scalar score (Du et al., 2025), hindering the surfacing of conflicting evidence and early correction of premature commitments, even with robust VLM backbones (Zhou et al., 2024b), causing the performance gap that is to be bridged in this paper. To overcome these limitations, this paper proposes a novel Dual-Stance Cooperative Debate Navigation (DSCD-Nav) framework (Fig. 1(c)) that mitigates overconfidence and weak self-correction in single-stream navigation pipelines.

Our DSCD-Nav advocates a stance-based cross-checking and evidence-aware arbitration mechanism that replaces traditional one-shot scoring in zero-shot indoor navigation, boosting action reliability under partial observability without modifying the underlying candidate generator or perception modules. Specifically, a Task–Scene Understanding agent (TSU) proposes a goal-progress action from the shared candidate set, while a Safety–Information Balancing agent (SIB) independently audits the proposal and can counter with a safer or more informative alternative. A Navigation Consensus Arbitration agent (NCA) then consolidates both sides’ reasons and evidence, optionally triggering lightweight micro-probing to verify uncertain choices. This design explicitly exposes and resolves candidate conflicts, producing actions that better balance progress, safety, and information gain. Overall, the main contributions of this work are as follows:

- We propose DSCD-Nav, a training-free dual-stance cooperative debate navigation framework featuring TSU and SIB agents that iteratively deliberate over shared candidate actions to balance goal progress and safety-aware information gain, effectively reducing overconfident decisions and serving as a plug-and-play add-on to existing VLM-based navigation pipelines.
- We propose a Navigation Consensus Arbitration (NCA) agent that softly arbitrates among diverse stance preferences based on task progress, safety, and information value. More significantly, when disagreement

persists but the top directions are geometrically close, we trigger lightweight micro-probing, executing small-stepping probes to validate uncertain choices for safer decisions with improved interpretability.

- Our experiments on ObjectNav and GOAT benchmarks demonstrate consistent gains in navigation success and efficiency, highlighting the practical value of dual-stance decision making, while the debate and arbitration traces provide clear, interpretable rationales for each action decision.

2. Related Work

2.1. Map-Centric Navigation and Frontier Exploration

Classical embodied navigation methods rely on explicit geometric and semantic representations, such as occupancy maps (Raychaudhuri & Chang, 2025), topological graphs (Yang et al., 2025; Chen et al., 2024), and object-level or open-vocabulary semantic maps (Busch et al., 2025; Jiang et al., 2025; Zhang et al., 2025a; Kuang et al., 2024), to support interpretable exploration and goal-directed search in unseen environments (Zhang et al., 2025b; Al-Halah et al., 2022; Xu et al., 2024; Wang et al., 2025d). While online scene graphs (Yin et al., 2024) and frontier-based reasoning (Yokoyama et al., 2024; Ramakrishnan et al., 2025) improve structured target search and efficiency, these pipelines remain tightly coupled to localization accuracy, semantic projection (Raychaudhuri & Chang, 2025; Xu et al., 2025), and handcrafted scoring rules. As a result, systematic representation bias is often propagated downstream, where decisions are made under a single, potentially flawed world model without action-level self-correction.

2.2. VLM and World-Model-Enhanced Navigation

Recent work brings VLM understanding (Goetting et al., 2024; Ling & Bai, 2025; Zhou et al., 2024a; Long et al., 2024; Yin et al., 2025) into candidate-action selection through iterative visual prompting (Nasiriany et al., 2024), and further augments decision-making with visual world models (Nie et al., 2025) or future-view prediction (Zhang et al., 2024a; Qin et al., 2025) for planning (Wang et al., 2023). These designs strengthen evidence–goal alignment (Rajabi & Kosecka, 2025) and improve robustness in complex, long-horizon settings via spatial reasoning (Zhong et al., 2025; Du et al., 2025) and memory signals (Cao et al., 2025; Zeng et al., 2025; Zhang et al., 2025c). Still, action choice often collapses to selecting a single best candidate (Gu et al., 2025), leaving evidence conflicts and efficiency, safety, or information-gain trade-offs largely implicit and allowing early bias to propagate across trajectories (Wang et al., 2025c).

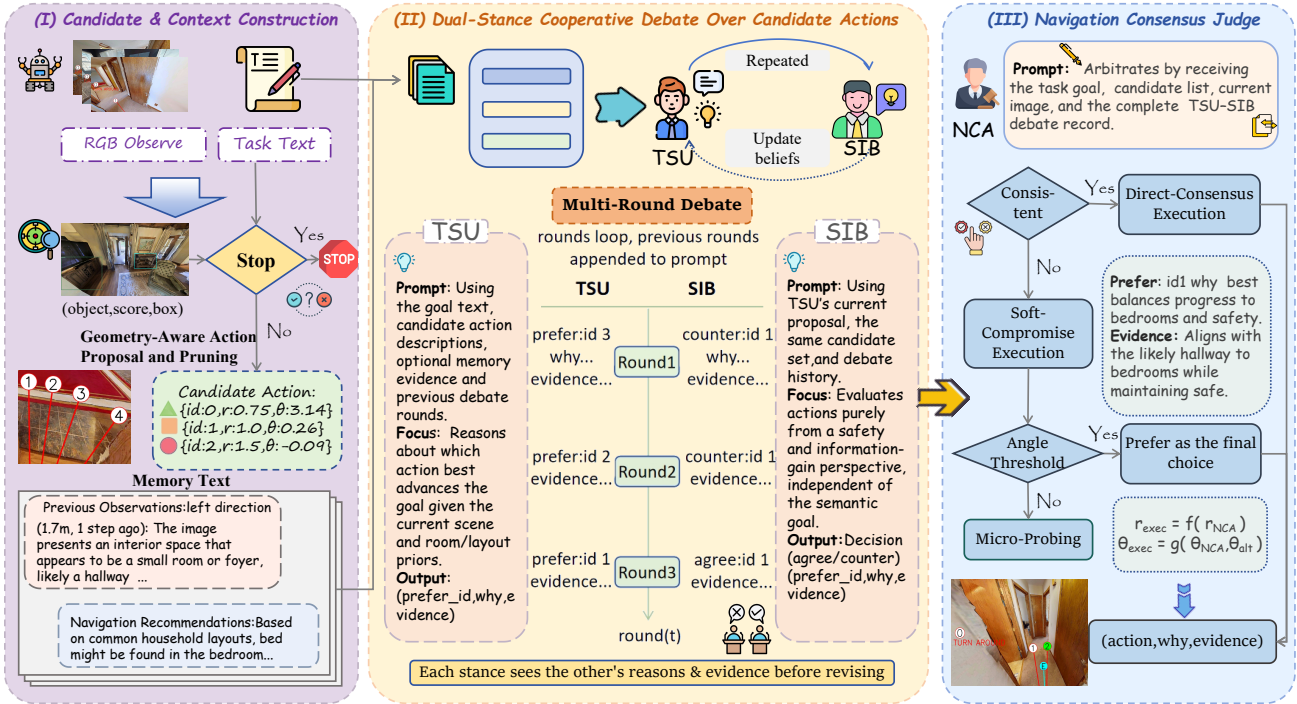


Figure 2. **DSCD-Nav overview.** (I) Candidate and context construction packages the goal, optional memory, and evidence cues, and a geometry-pruned set of executable polar action candidates with language descriptions into debate-ready inputs. (II) TSU and SIB conduct multi-round cooperative debate over the shared candidates, exchanging preferences and cue-grounded evidence while updating beliefs. (III) The NCA judge arbitrates the debate to produce a final action with a concise rationale and supporting evidence, after which the system executes it directly under consensus or applies bounded geometric soft-compromise with micro-probing when disagreement persists, and the angular gap is within a preset threshold.

2.3. Multi-Agent Debate and Consensus Decision

In multi-agent debate, voting, and judge-based frameworks (Estornell & Liu, 2024; Choi et al., 2025; Kaesberg et al., 2025), agents with different stances exchange reasons and evidence over the same query; a consensus or arbitration module then aggregates their views (Wang et al., 2025b) to reduce overconfidence (Lin & Hooi, 2025) and make disagreements explicit (Liang et al., 2024). In embodied and robotic settings, work on LLM-driven multi-agent coordination (Zhang et al., 2025d) and long-horizon planning (Nayak et al., 2024; Wang et al., 2025a) informs action decision-making. However, existing debate and consensus methods are mostly confined to textual reasoning or high-level plans (Becker et al., 2025), with limited focus on the candidate-action layer in 3D navigation, where errors compound; thus, action-level dual-stance cross-checking and arbitration remain underexplored.

3. Method

Task Definition. We consider *zero-shot 3D indoor object navigation* (Batra et al., 2020), where an agent receives first-

person observations o_t and target semantic text g at each discrete time step t . Let the true environment state be s_t , after executing an action a_t , the state evolves according to a Markovian transition $s_{t+1} \sim \mathcal{T}(s_t, a_t)$. The episode ends when the agent executes STOP or reaches a maximum step budget, and success is achieved if STOP is called when the agent is within a success radius of the target object.

Method Overview. We propose the Dual-Stance Cooperative Debate Navigation framework (DSCD-Nav), illustrated in Fig. 2. At each time step, we take the candidate set \mathcal{A}_t as a unified interface: without changing the underlying generator, we only apply a lightweight wrapper to form debate-ready candidate cards \mathcal{C}_t , and assemble them with the goal text and optional weak evidence context \mathcal{E}_t to form $X_t = (g, \mathcal{C}_t, \mathcal{E}_t)$. Next, the TSU-Agent evaluates the same candidate set from the goal progress stance of task and scene understanding, producing a preferred proposal and supporting evidence. The SIB-Agent, from a task-agnostic safety-information stance emphasizing safety and information visibility, responds in an agree or counter manner and may propose safer or more informative alternatives. Multi-

round interaction yields a structured debate trace \mathcal{D}_t . The NCA-Agent then reads \mathcal{C}_t and \mathcal{D}_t and produces a final action identity with a unified, evidence-grounded rationale. Finally, we adopt a two-mode execution strategy: when the two stances converge, we directly execute the consensus action; when disagreement persists yet geometric directions remain amenable to compromise, we preserve the NCA selected high-level identity and apply soft preference with micro-probing at the geometric level via shorter steps and slight yaw bias, enabling low-risk validation of conflicting preferences.

3.1. Candidate Action and Context Interface

To avoid assuming a fixed discrete action set, we represent executable actions in continuous polar form. At each step t , an upstream candidate generator provides a set of feasible actions:

$$\mathcal{A}_t = \{a_i^t\}_{i=1}^{N_t}, \quad a_i^t = (r_i^t, \theta_i^t), \quad (1)$$

where (r_i^t, θ_i^t) are the forward distance and yaw offset relative to the agent’s current heading of candidate i at step t , with $i \in \{1, \dots, N_t\}$ and N_t the number of Geometry-Aware proposed candidates at step t .

DSCD-Nav operates purely at the decision layer and does not modify how \mathcal{A}_t is generated. We apply a lightweight packaging operator $\Phi(\mathcal{A}_t) \rightarrow \mathcal{C}_t$ to convert candidates into debate-ready cards with stable within-step identities:

$$\mathcal{C}_t = \{c_i^t\}_{i=1}^{N_t}, \quad c_i^t = (id_i^t, r_i^t, \theta_i^t, d_i^t), \quad (2)$$

where id_i^t is a step-local candidate identity used for cross-stance alignment at step t , and d_i^t is a machine-readable direction text for a_i^t . The operator $\Phi(\cdot)$ performs no re-scoring and only standardizes formatting to enable consistent comparison across agents. We optionally provide auxiliary evidence \mathcal{E}_t (e.g., brief memory cues) for prompting, and the per-step input to DSCD-Nav is $X_t = (g, \mathcal{C}_t, \mathcal{E}_t)$. Thus, DSCD-Nav introduces no additional sensors, training, or supervision, and only redefines how candidates are evaluated and selected to determine the final action.

3.2. Dual-Stance Cooperative Debate

We replace single-view candidate scoring with a cooperative debate between two complementary stances over the same candidate set. At each round k , TSU-Agent and SIB-Agent read each other’s previous reasons and evidence, and update their action preferences interactively.

To model the coupling between evidence and preference, we introduce a Bayesian-style *implicit belief* view. Given candidates \mathcal{A}_t at step t , each stance produces an evidence subset per round, denoted $ev_{\text{TSU}}^{(k)}$ and $ev_{\text{SIB}}^{(k)}$. Across rounds, evidence induces a structured relation set $\mathcal{R}^{(k)} = \mathcal{R}_{\text{sup}}^{(k)} \cup \mathcal{R}_{\text{att}}^{(k)}$, where $\mathcal{R}_{\text{sup}}^{(k)}$ supports candidate actions and $\mathcal{R}_{\text{att}}^{(k)}$ rebuts (or

weakens) the other stance’s previous preference and its supporting evidence. Each relation in $\mathcal{R}^{(k)}$ is a natural-language support or rebuttal statement grounded in visual evidence and candidate identities.

We denote the implicit belief states over candidates as $B_{\text{TSU}}^{(k)}$ and $B_{\text{SIB}}^{(k)}$. Their interactive evolution is abstracted by:

$$B_{\text{TSU}}^{(k)} = \text{Update}\left(B_{\text{TSU}}^{(k-1)}, ev_{\text{TSU}}^{(k)}, ev_{\text{SIB}}^{(k-1)}, \mathcal{R}^{(k)}\right), \quad (3)$$

$$B_{\text{SIB}}^{(k)} = \text{Update}\left(B_{\text{SIB}}^{(k-1)}, ev_{\text{SIB}}^{(k)}, ev_{\text{TSU}}^{(k-1)}, \mathcal{R}^{(k)}\right). \quad (4)$$

Here, $\text{Update}(\cdot)$ is an abstract operator implemented implicitly via next-round prompting, not an explicit analytical rule. When supportive relations dominate, the two stances tend to align; otherwise, persistent attacks maintain a structured disagreement, which is then resolved by NCA arbitration and used to trigger execution-mode switching.

3.2.1. TSU-AGENT: TASK-SCENE UNDERSTANDING

TSU-Agent is an explicitly goal-aware stance that prioritizes *goal progress* and *scene understanding*. Given the shared candidates, TSU treats the goal semantics g as the primary constraint and combines the current observation with historical context to infer which directions are most likely to reach the target. Beyond local geometric feasibility, TSU leverages layout cues and commonsense room-object associations to form a task-driven preference over candidates. When weak evidence \mathcal{E}_t is available, TSU uses it as auxiliary support to refine or strengthen its hypothesis.

In round k of the debate, TSU outputs a preferred candidate with a brief rationale and supporting evidence:

$$(id_{\text{TSU}}^{(k)}, w_{\text{TSU}}^{(k)}, ev_{\text{TSU}}^{(k)}) = f_{\text{TSU}}(X_t, \mathcal{H}^{(k-1)}), \quad (5)$$

where $f_{\text{TSU}}(\cdot)$ denotes the TSU inference policy, and $\mathcal{H}^{(k-1)}$ summarizes the dialogue history up to round $k-1$ (including SIB’s counters and TSU’s previous choices). Concretely, TSU returns (1) a single preferred candidate $id_{\text{TSU}}^{(k)}$, (2) a concise *why* $w_{\text{TSU}}^{(k)}$, and (3) evidence snippets $ev_{\text{TSU}}^{(k)}$ supporting goal-advancing and layout-consistent navigation. TSU thus anchors the debate with a task-driven proposal.

3.2.2. SIB-AGENT: SAFETY-INFORMATION BALANCING

SIB-Agent adopts an explicitly task-agnostic stance centered on *safety* and *information utility*. It does not infer goal-directed actions from g ; instead, it audits TSU’s proposal and the shared candidates under risk and observability constraints, discouraging overconfident commitments. When TSU’s preferred action may incur collision risk, uncertain narrow-space traversal, poor visibility, or premature directional commitment, SIB issues a *counter* and recommends a



Figure 3. Qualitative case study on HM3Dv2 ObjectNav. We overlay the executed trajectory on the reconstructed 3D scene and annotate several decision points with the corresponding TSU and SIB preferences and the NCA arbitration result. The trace highlights DSCD-Nav’s ability to resolve disagreement at visually ambiguous viewpoints and, when needed, trigger a conservative micro-probing step before committing to the executed action.

safer or more informative alternative that expands viewpoint coverage.

In debate round k , SIB outputs an *agree/counter* decision, an (optional) alternative candidate, and supporting rationale:

$$(dec^{(k)}, id_{SIB}^{(k)}, w_{SIB}^{(k)}, ev_{SIB}^{(k)}) = f_{SIB}(X_t, id_{TSU}^{(k)}, \mathcal{H}^{(k-1)}), \quad (6)$$

where $dec^{(k)} \in \{\text{agree}, \text{counter}\}$ and $\mathcal{H}^{(k-1)}$ is the dialogue history up to round $k-1$. If $dec^{(k)} = \text{counter}$, SIB proposes $id_{SIB}^{(k)}$ with concise evidence grounded in local traversability, risk reduction, and expected observability gain, rather than goal semantics. This task-agnostic stance provides a structured counterbalance that complements TSU and enriches the evidence space for arbitration.

3.2.3. STRUCTURED DEBATE TRACE

After K rounds, we obtain a structured debate trace:

$$\mathcal{D}_t = \left\{ (id_{TSU}^{(k)}, w_{TSU}^{(k)}, ev_{TSU}^{(k)}, dec^{(k)}, id_{SIB}^{(k)}, w_{SIB}^{(k)}, ev_{SIB}^{(k)}) \right\}_{k=1}^K. \quad (7)$$

Unlike score-fusion methods that aggregate independent decision signals, DSCD-Nav keeps a shared candidate set and enforces explicit exchange of reasons and evidence, so preferences either converge through interaction or remain as a structured disagreement for arbitration and execution-mode switching. We also log \mathcal{D}_t and the final decision id^* (with flags for soft compromise and micro-probing), forming a step-wise evidence–action trace for ablation and failure-case analysis.

3.3. Two-Mode Execution Policy

To unify dual-stance outputs into an executable action, we introduce NCA-Agent to arbitrate the debate trace and trigger a two-mode execution policy. Specifically, we define a consensus indicator based on final-round agreement:

$$\mathbb{I}_t^{\text{cons}} = \mathbb{I} [dec^{(K)} = \text{agree}], \quad (8)$$

where $\mathbb{I}[\cdot]$ is the indicator function (1 if the condition holds, 0 otherwise). The execution mode is selected as:

$$\begin{cases} \text{Mode B} & \text{if } \mathbb{I}_t^{\text{cons}} = 0 \wedge |\Delta\theta| \leq \alpha, \\ \text{Mode A} & \text{otherwise,} \end{cases} \quad (9)$$

Example 8-step Debate-Guided ObjectNav Trajectory

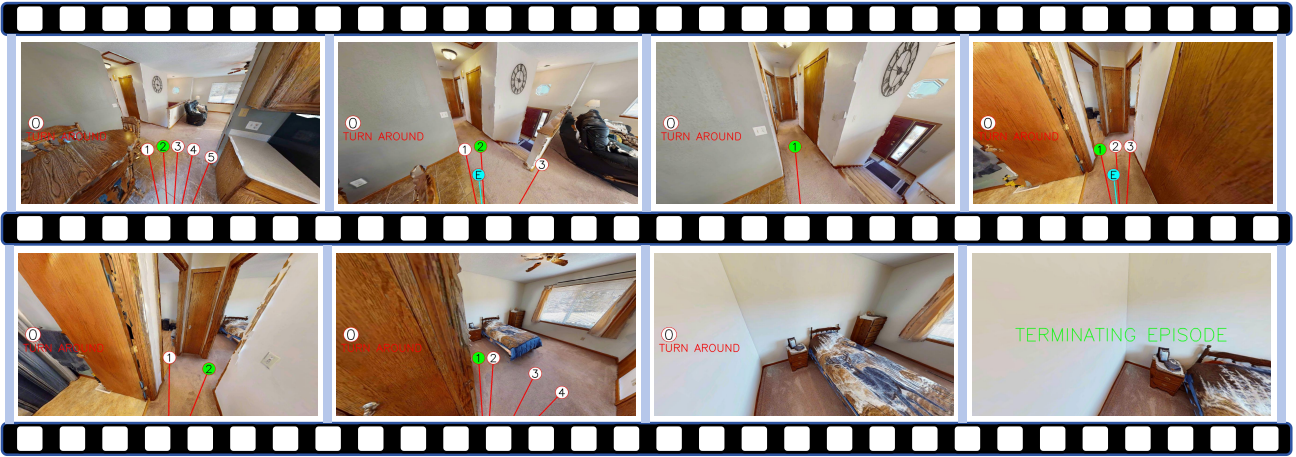


Figure 4. An 8-step, debate-guided HM3Dv1 ObjectNav episode from the agent’s first-person view, illustrating sequential observations, executed actions, and successful termination at the target.

where θ^* denotes the yaw angle of the NCA-arbitrated action, θ^{alt} denotes the yaw angle of the other stance’s final preferred candidate, and $\Delta\theta = \text{wrap}(\theta^{\text{alt}} - \theta^*) \in (-\pi, \pi]$ is the signed shortest angular difference (wrapped to the principal interval); α is the compromise threshold. Mode A commits to executing the NCA-arbitrated candidate id^* for decision stability, while Mode B triggers a conservative soft-compromise procedure when disagreement is small.

3.3.1. NCA-AGENT: UNIFIED ARBITRATION

NCA-Agent reads \mathcal{C}_t and the full debate trace \mathcal{D}_t to produce a stance-agnostic, evidence-aware final decision:

$$(id^*, w^*, ev^*) = f_{\text{NCA}}(g, \mathcal{C}_t, \mathcal{D}_t). \quad (10)$$

Here, id^* is the final high-level action identity, and w^* and ev^* are concise summaries distilled from both stances’ arguments. We denote the geometry associated with id^* as $a^* = (r^*, \theta^*)$. NCA does not simply pick a “winner”. Instead, it evaluates proposals under a unified set of criteria aligned with task progress, safety, and information considerations, producing an interpretable consensus action.

3.3.2. MODE A: DIRECT-CONSENSUS EXECUTION

When the two stances converge in the final round, or SIB explicitly agrees with TSU’s proposal, we directly execute the geometric parameters associated with id^* :

$$(r_{\text{exec}}, \theta_{\text{exec}}) = (r^*, \theta^*). \quad (11)$$

This mode preserves execution simplicity while retaining interpretability through w^* and ev^* .

3.3.3. MODE B: SOFT-COMPROMISE AND MICRO-PROBING

When disagreement persists after multi-round debate, we check whether the two final preferences are geometrically close enough for a safe compromise. We define:

$$a^* = (r^*, \theta^*), \quad a^{\text{alt}} = (r^{\text{alt}}, \theta^{\text{alt}}), \quad (12)$$

where a^{alt} denotes the alternative preferred by the other stance in the last round. If $|\Delta\theta| \leq \alpha$, we apply a geometric soft-compromise consistent with our implementation: the high-level identity remains id^* , while the low-level execution is adjusted via shortened forward motion and a slight yaw bias toward the alternative direction:

$$r_{\text{exec}} = \beta_r r^*, \quad \theta_{\text{exec}} = \theta^* + \beta_\theta \Delta\theta. \quad (13)$$

We implement Mode B as a micro-probing step parameterized by (β_r, β_θ) , where β_r scales the forward motion and β_θ interpolates the yaw toward the alternative direction. This micro-probing step keeps the execution close to a^* while inducing a controlled viewpoint change to acquire disambiguating evidence at ambiguous junctions. After executing the micro-probing step, the next step re-enters the debate–arbitration pipeline with the newly acquired observation, enabling evidence accumulation before hard commitment. It preserves the NCA-selected primary heading, yet expands the immediate observation to evaluate the alternative’s expected information gain and safety balance. We use $(\beta_r, \beta_\theta) = (\frac{1}{2}, \frac{1}{3})$ by default, and report a sensitivity analysis in Appendix A.3. If the directional gap exceeds the threshold α , we execute the NCA-arbitrated action a^* (Mode A) to avoid instability from overly aggressive compromise.

Table 1. Comprehensive comparison with state-of-the-art methods on ObjectNav benchmarks. TF denotes training-free, and ZS denotes zero-shot. Our method uses the lightweight Gemini-2.5-Flash-Lite as the base VLM.

Method	ZS	TF	HM3Dv1		HM3Dv2		MP3D	
			SR(%) ↑	SPL(%) ↑	SR(%) ↑	SPL(%) ↑	SR(%) ↑	SPL(%) ↑
SemEXP (Chaplot et al., 2020)	×	×	–	–	–	–	36.0	14.4
ProcTHOR (Deitke et al., 2022)	×	×	54.4	31.8	–	–	–	–
ZSON (Majumdar et al., 2022)	×	×	25.5	12.6	–	–	15.3	4.8
PONI (Ramakrishnan et al., 2022)	×	×	–	–	–	–	31.8	12.1
PSL (Sun et al., 2024)	×	×	42.4	19.2	–	–	–	–
Habitat-Web (Ramrakhya et al., 2022)	✓	×	41.5	16.0	–	–	31.6	8.5
ProcTHOR-ZS (Deitke et al., 2022)	✓	×	13.2	7.7	–	–	–	–
Pixel-Nav (Cai et al., 2024)	✓	×	37.9	20.5	–	–	–	–
SGM (Zhang et al., 2024c)	✓	×	60.2	30.8	–	–	37.7	14.7
VLFM (Yokoyama et al., 2024)	✓	×	52.5	30.4	63.6	32.5	36.4	17.5
CoW (Gadre et al., 2023)	✓	✓	–	–	–	–	7.4	3.7
ESC (Zhou et al., 2023)	✓	✓	39.2	22.3	–	–	28.7	14.2
L3MVN (Yu et al., 2023)	✓	✓	50.4	23.1	36.3	15.7	34.9	14.5
TriHelper (Zhang et al., 2024b)	✓	✓	62.0	25.3	–	–	–	–
OpenFMNav (Kuang et al., 2024)	✓	✓	51.9	24.4	–	–	37.2	15.7
InstructNav (Long et al., 2024)	✓	✓	–	–	58.0	20.9	–	–
SG-Nav (Yin et al., 2024)	✓	✓	54.0	24.9	49.6	25.5	40.2	16.0
OneMap (Busch et al., 2025)	✓	✓	55.8	37.4	–	–	–	–
TopV-Nav (Zhong et al., 2025)	✓	✓	52.0	28.6	–	–	35.2	16.4
CogNav (Cao et al., 2025)	✓	✓	72.5	26.2	–	–	46.6	16.1
DSCD (Ours)	✓	✓	75.6	40.1	73.0	38.7	47.8	24.2

4. Experiment

4.1. Experiment Setup

Datasets. We evaluate in Habitat on the validation splits of HM3Dv1 (Ramakrishnan et al., 2021), HM3Dv2 (Yadav et al., 2023), and MP3D ObjectNav (Chang et al., 2017), and further adopt GOAT (a multimodal lifelong navigation benchmark built on HM3Dv1) (Khanna et al., 2024). These benchmarks support fair comparison on standard ObjectNav settings and test whether dual-stance debate with consensus arbitration mitigates overconfident decisions and redundant exploration in longer-horizon, multi-subgoal navigation.

Implementation Details. The action set includes `stop`, `rotate`, and `move_forward`, where the forward distance is sampled from a continuous range [0.4 m, 1.5 m] to balance long strides and local probing. DSCD-Nav employs the lightweight Gemini-2.5-Flash-Lite as its vision-language backbone. For fair comparison, we keep the candidate generator and perception settings identical to the baselines, and only replace the action-selection policy with our dual-stance debate and consensus arbitration.

Evaluation Metrics. We evaluate using Success Rate (SR), Success weighted by Path Length (SPL), and the Area Overlap Redundancy Index (AORI). SR is the fraction of episodes where the agent stops successfully near the target. SPL measures path efficiency by comparing shortest-path length to the executed path length on successful episodes.

AORI quantifies exploration redundancy by penalizing revisits to previously covered areas (lower is better). Formal definitions are provided in Appendix A.4.

4.2. Methods Comparison

4.2.1. QUALITATIVE ANALYSIS

As shown in Fig. 3, DSCD-Nav avoids premature commitment at visually ambiguous junctions by balancing TSU and SIB stances through debate and NCA arbitration, with conservative micro-probing when needed, reducing detours along the trajectory. Fig. 4 further provides a first-person trace, illustrating how debate-informed decisions evolve over sequential observations and lead to timely termination once target evidence is confirmed.

4.2.2. QUANTITATIVE ANALYSIS

We evaluate on ObjectNav in HM3Dv1, HM3Dv2, and MP3D, and compare against state-of-the-art methods in Table 1. DSCD-Nav achieves higher SR and SPL across all three benchmarks, indicating improved success and efficiency. The results suggest that structured dual-stance decision making yields more robust candidate selection in complex indoor scenes and transfers across datasets.

Furthermore, we compare our method with other representative prompt-only baselines on HM3Dv2 (ObjectNav, val; Table 2(a)) and HM3Dv1 (GOAT, val unseen; Table 2(b)), with results reported in Table 2. Our method improves the

performance of prompt-based approaches and is consistent with the conclusions on ObjectNav. On GOAT, it also boosts SR and SPL while significantly reducing AORI, indicating that it can maintain more stable progress and lower exploration redundancy in multi-subgoal, long-horizon tasks.

Table 2. Comparison of training-free prompt-based navigation methods on ObjectNav and GOAT benchmarks.

(a) ObjectNav benchmark			
Method	SR (%) \uparrow	SPL (%) \uparrow	AORI (%) \downarrow
Prompt-only	29.8	10.7	–
PIVOT	24.6	10.6	63.3
VLMNav	51.6	18.3	61.5
DORAEMON	62.0	23.0	50.1
DSCD (Ours)	73.0	38.7	39.2
(b) GOAT benchmark			
Method	SR (%) \uparrow	SPL (%) \uparrow	AORI (%) \downarrow
Prompt-only	11.3	3.7	–
PIVOT	8.3	3.8	64.9
VLMNav	22.1	9.3	63.6
DORAEMON	24.3	10.3	56.9
DSCD (Ours)	40.1	32.3	41.9

4.3. Ablation Study

We conduct comprehensive ablation studies to validate the design choices of DSCD-Nav, with results summarized in Table 3.

Table 3. Ablation studies of DSCD modules, debate rounds, and backbone VLMs on HM3Dv2 ObjectNav benchmark.

Method / Configuration	SR (%) \uparrow	SPL (%) \uparrow	AORI (%) \downarrow
(a) Ablation of DSCD modules			
TSU-only	62.4	27.6	49.5
SIB-only	56.5	25.9	44.1
w/o NCA-Agent	67.8	33.8	43.2
w/o micro-probing	71.2	36.9	41.0
DSCD (Ours, default)	73.0	38.7	39.2
(b) Ablation of debate rounds			
rounds = 1	51.3	30.8	45.0
rounds = 2	65.6	36.7	41.0
rounds = 3 (default)	73.0	38.7	39.2
rounds = 4	73.1	38.7	38.9
(c) Ablation of different VLMs			
Gemini-2.5-Flash	80.1	41.1	36.1
Gemini-2.5-Flash-Lite	73.0	38.7	39.2
GPT-4.1-nano	58.7	29.9	50.5

(a) Core components. Removing either TSU or SIB consistently degrades performance. Without TSU, the agent loses goal-directed guidance and scene-semantic alignment;

without SIB, the risk-information counterbalance disappears. Removing NCA further eliminates unified arbitration under disagreement, making the final action more susceptible to single-stance bias. Disabling micro-probing reduces low-cost verification during disagreement and tends to increase AORI or reduce SPL.

(b) Debate rounds. Table 3(b) shows that using more debate rounds generally improves decision quality by enabling richer interaction and evidence refinement. However, the marginal gains saturate as rounds increase, while inference cost grows, so we adopt a default setting that balances performance and efficiency.

(c) Choice of VLM. As shown in Table 3(c), absolute performance varies across VLM backbones, but DSCD-Nav remains strong even with the lightweight Gemini-2.5-Flash-Lite. This indicates that the improvements mainly stem from the decision structure rather than a specific backbone model.

Table 4. Comparison of disagreement-related debate metrics and Δ SPL across Single-Stance Self-Debate (SSSD) and DSCD configurations. Metric calculation formulas are provided in Appendix A.4.

Config	DR (%)	JOR (%)	MPTR (%)	Δ SPL \uparrow
SSSD	5.0	60.0	20.0	–
DSCD, rounds=1	41.0	43.0	41.0	7.1
DSCD, rounds=2	21.4	45.5	63.6	18.4
DSCD, rounds=3	15.6	50.0	20.0	20.3

To interpret DSCD-Nav at the process level, Table 4 summarizes key disagreement statistics, including the Disagreement Rate (DR) over candidate preferences, the Judge Override Rate (JOR) during arbitration, and the Micro-Probing Trigger Rate (MPTR) when final-round stances disagree. Overall, disagreements concentrate at high-uncertainty steps and reflect explicit candidate conflicts rather than random noise. Arbitration and micro-probing then convert these conflicts into more robust actions, consistent with the gains in SPL.

5. Conclusion

In this paper, we propose DSCD-Nav, a training-free dual-stance cooperative debate framework where TSU and SIB cross-check shared candidate actions under partial observability. NCA arbitration integrates both stances into a final action, with lightweight micro-probing triggered under persistent near-direction disagreement to validate competing preferences at low risk. Experiments on ObjectNav and GOAT show consistent gains in success and path efficiency with reduced exploration redundancy, and ablations verify each component.

References

- Al-Halah, Z., Ramakrishnan, S. K., and Grauman, K. Zero experience required: Plug & play modular transfer learning for semantic visual navigation. In *Proceedings of the IEEE/CVF Conference on Computer Vision and Pattern Recognition (CVPR)*, pp. 17031–17041, 2022.
- Batra, D., Gokaslan, A., Kembhavi, A., Maksymets, O., Mottaghi, R., Savva, M., Toshev, A., and Wijmans, E. ObjectNav Revisited: On evaluation of embodied agents navigating to objects. *arXiv preprint arXiv:2006.13171*, 2020.
- Becker, J., Kaesberg, L. B., Bauer, N., Wahle, J. P., Ruas, T., and Gipp, B. MALLM: Multi-agent large language models framework. In *Proceedings of the 2025 Conference on Empirical Methods in Natural Language Processing: System Demonstrations*, pp. 418–439, 2025.
- Busch, F. L., Homberger, T., Ortega-Peimbert, J., Yang, Q., and Andersson, O. One map to find them all: Real-time open-vocabulary mapping for zero-shot multi-object navigation. In *Proceedings of the IEEE International Conference on Robotics and Automation (ICRA)*, pp. 14835–14842, 2025.
- Cai, W., Huang, S., Cheng, G., Long, Y., Gao, P., Sun, C., and Dong, H. Bridging zero-shot object navigation and foundation models through pixel-guided navigation skill. In *Proceedings of the IEEE International Conference on Robotics and Automation (ICRA)*, pp. 5228–5234, 2024.
- Cao, Y., Zhang, J., Yu, Z., Liu, S., Qin, Z., Zou, Q., Du, B., and Xu, K. CogNav: Cognitive process modeling for object goal navigation with LLMs. In *Proceedings of the IEEE/CVF International Conference on Computer Vision*, pp. 9550–9560, 2025.
- Chang, A., Dai, A., Funkhouser, T., Halber, M., Niebner, M., Savva, M., Song, S., Zeng, A., and Zhang, Y. Matterport3D: Learning from RGB-D data in indoor environments. In *International Conference on 3D Vision (3DV)*, 2017.
- Chaplot, D. S., Gandhi, D. P., Gupta, A., and Salakhutdinov, R. R. Object goal navigation using goal-oriented semantic exploration. In *Advances in Neural Information Processing Systems*, volume 33, pp. 4247–4258, 2020.
- Chen, J., Lin, B., Xu, R., Chai, Z., Liang, X., and Wong, K.-Y. MapGPT: Map-guided prompting with adaptive path planning for vision-and-language navigation. In *Proceedings of the 62nd Annual Meeting of the Association for Computational Linguistics*, pp. 9796–9810, 2024.
- Choi, H. K., Zhu, J., and Li, S. Debate or vote: Which yields better decisions in multi-agent large language models? In *Advances in Neural Information Processing Systems*, 2025.
- Deitke, M., VanderBilt, E., Herrasti, A., Weihs, L., Ehsani, K., Salvador, J., Han, W., Kolve, E., Kembhavi, A., and Mottaghi, R. ProcTHOR: Large-scale embodied AI using procedural generation. In *Advances in Neural Information Processing Systems*, volume 35, pp. 5982–5994, 2022.
- Du, Y., Fu, T., Chen, Z., Li, B., Su, S., Zhao, Z., and Wang, C. VL-Nav: Real-time vision-language navigation with spatial reasoning. *arXiv preprint arXiv:2502.00931*, 2025.
- Estornell, A. and Liu, Y. Multi-LLM debate: Framework, principals, and interventions. In *Advances in Neural Information Processing Systems*, 2024.
- Gadre, S. Y., Wortsman, M., Ilharco, G., Schmidt, L., and Song, S. Cows on pasture: Baselines and benchmarks for language-driven zero-shot object navigation. In *Proceedings of the IEEE/CVF Conference on Computer Vision and Pattern Recognition (CVPR)*, pp. 23171–23181, 2023.
- Goetting, D., Singh, H. G., and Loquercio, A. End-to-end navigation with vision language models: Transforming spatial reasoning into question-answering. *arXiv preprint arXiv:2411.05755*, 2024.
- Gu, T., Li, L., Wang, X., Gong, C., Gong, J., Zhang, Z., Xie, Y., Ma, L., and Tan, X. DORAEMON: Decentralized ontology-aware reliable agent with enhanced memory oriented navigation. *arXiv preprint arXiv:2505.21969*, 2025.
- Jiang, J., Zhu, Y., Wu, Z., and Song, J. Dualmap: Online open-vocabulary semantic mapping for natural language navigation. *IEEE Robotics and Automation Letters*, 10 (12):12612–12619, 2025.
- Kaesberg, L. B., Becker, J., Wahle, J. P., Ruas, T., and Gipp, B. Voting or consensus? decision-making in multi-agent debate. In *Findings of the Association for Computational Linguistics: ACL 2025*, pp. 11640–11671, 2025.
- Khanna, M., Ramrakhya, R., Chhablani, G., Yenamandra, S., Gervet, T., Chang, M., Kira, Z., Chaplot, D. S., Batra, D., and Mottaghi, R. GOAT-bench: A benchmark for multi-modal lifelong navigation. In *Proceedings of the IEEE/CVF Conference on Computer Vision and Pattern Recognition (CVPR)*, 2024.
- Kuang, Y., Lin, H., and Jiang, M. OpenFMNav: Towards open-set zero-shot object navigation via vision-language foundation models. In *Findings of the Association for Computational Linguistics: NAACL 2024*, pp. 338–351, 2024.

- Liang, T., He, Z., Jiao, W., Wang, X., Wang, Y., Wang, R., Yang, Y., Shi, S., and Tu, Z. Encouraging divergent thinking in large language models through multi-agent debate. In *Proceedings of the 2024 Conference on Empirical Methods in Natural Language Processing*, pp. 17889–17904, 2024.
- Lin, Z. and Hooi, B. Enhancing multi-agent debate system performance via confidence expression. In *Findings of the Association for Computational Linguistics: EMNLP 2025*, pp. 6453–6471, 2025.
- Ling, L. and Bai, Q. Endowing embodied agents with spatial reasoning capabilities for vision-and-language navigation. *arXiv preprint arXiv:2504.08806*, 2025.
- Long, Y., Cai, W., Wang, H., Zhan, G., and Dong, H. InstructNav: Zero-shot system for generic instruction navigation in unexplored environment. In *Proceedings of the Conference on Robot Learning (CoRL)*, 2024.
- Majumdar, A., Aggarwal, G., Devnani, B., Hoffman, J., and Batra, D. ZSON: Zero-shot object-goal navigation using multimodal goal embeddings. In *Advances in Neural Information Processing Systems*, volume 35, pp. 32340–32352, 2022.
- Nasiriany, S., Xia, F., Yu, W., Xiao, T., Liang, J., Dasgupta, I., Xie, A., Driess, D., Wahid, A., Xu, Z., Vuong, Q., Zhang, T., Lee, T.-W. E., Lee, K.-H., Xu, P., Kirmani, S., Zhu, Y., Zeng, A., Hausman, K., Heess, N., Finn, C., Levine, S., and Ichter, B. PIVOT: Iterative visual prompting elicits actionable knowledge for VLMs. In *Workshop on Vision-Language Models for Navigation and Manipulation at ICRA*, 2024.
- Nayak, S., Orozco, A. M., Have, M. T., Thirumalai, V., Zhang, J., Chen, D., Kapoor, A., Robinson, E., Gopalakrishnan, K., Harrison, J., Ichter, B., Mahajan, A., and Balakrishnan, H. Long-horizon planning for multi-agent robots in partially observable environments. In *Advances in Neural Information Processing Systems*, volume 37, pp. 67929–67967, 2024.
- Nie, D., Guo, X., Duan, Y., Zhang, R., and Chen, L. WM-Nav: Integrating vision-language models into world models for object goal navigation. In *Proceedings of the IEEE/RSJ International Conference on Intelligent Robots and Systems (IROS)*, pp. 2392–2399, 2025.
- Qin, Y., Sun, A., Hong, Y., Wang, B., and Zhang, R. NavigateDiff: Visual predictors are zero-shot navigation assistants. In *Proceedings of the IEEE International Conference on Robotics and Automation (ICRA)*, pp. 12002, 2025.
- Rajabi, N. and Kosecka, J. TRAVEL: Training-free retrieval and alignment for vision-and-language navigation. In *Workshop on Foundation Models Meet Embodied Agents at CVPR*, 2025.
- Ramakrishnan, S. K., Gokaslan, A., Wijmans, E., Maksymets, O., Clegg, A., Turner, J., Undersander, E., Galuba, W., Westbury, A., Chang, A., Savva, M., Zhao, Y., and Batra, D. Habitat-matterport 3D dataset (HM3D): 1000 large-scale 3D environments for embodied AI. In *Proceedings of the NeurIPS Track on Datasets and Benchmarks*, 2021.
- Ramakrishnan, S. K., Chaplot, D. S., Al-Halah, Z., Malik, J., and Grauman, K. PONI: Potential functions for objectgoal navigation with interaction-free learning. In *Proceedings of the IEEE/CVF Conference on Computer Vision and Pattern Recognition (CVPR)*, pp. 18890–18900, 2022.
- Ramakrishnan, S. K., Wijmans, E., Kraehenbuehl, P., and Koltun, V. Does spatial cognition emerge in frontier models? In *Proceedings of the International Conference on Learning Representations*, 2025.
- Ramrakhya, R., Undersander, E., Batra, D., and Das, A. Habitat-Web: Learning embodied object-search strategies from human demonstrations at scale. In *Proceedings of the IEEE/CVF Conference on Computer Vision and Pattern Recognition (CVPR)*, pp. 5173–5183, 2022.
- Raychaudhuri, S. and Chang, A. X. Semantic mapping in indoor embodied AI - a survey on advances, challenges, and future directions. *Transactions on Machine Learning Research*, 2025. ISSN 2835-8856.
- Sun, X., Liu, L., Zhi, H., Qiu, R., and Liang, J. Prioritized semantic learning for zero-shot instance navigation. In *Proceedings of the European Conference on Computer Vision (ECCV)*, pp. 161–178, 2024.
- Wang, H., Liang, W., Van Gool, L., and Wang, W. Dreamwalker: Mental planning for continuous vision-language navigation. In *Proceedings of the IEEE/CVF International Conference on Computer Vision*, pp. 10873–10883, 2023.
- Wang, W., Obi, I., and Min, B.-C. Multi-agent LLM actor-critic framework for social robot navigation. *arXiv preprint arXiv:2503.09758*, 2025a.
- Wang, X., Wang, J., Wang, Y., Dang, P., Cao, S., and Zhang, C. MARS: toward more efficient multi-agent collaboration for LLM reasoning. *arXiv preprint arXiv:2509.20502*, 2025b.

- Wang, Z., Lee, S., and Lee, G. H. Dynam3D: Dynamic layered 3D tokens empower VLM for vision-and-language navigation. In *Advances in Neural Information Processing Systems*, 2025c.
- Wang, Z., Liu, Y., Cheng, X., and Ikenaga, T. MIRROR: Multiple indoor rooms reconstruction with optimized refinement from monocular videos. *IEICE Transactions on Information and Systems*, 2025d.
- Wu, Z., Wang, Z., Xu, X., Yin, H., Liang, Y., Ma, A., Lu, J., and Yan, H. Embodied instruction following in unknown environments. In *Proceedings of the IEEE/RSJ International Conference on Intelligent Robots and Systems (IROS)*, pp. 21825–21832, 2025.
- Xu, X., Xia, C., Wang, Z., Zhao, L., Duan, Y., Zhou, J., and Lu, J. Memory-based adapters for online 3D scene perception. In *Proceedings of the IEEE/CVF Conference on Computer Vision and Pattern Recognition (CVPR)*, pp. 21604–21613, 2024.
- Xu, X., Chen, H., Zhao, L., Wang, Z., Zhou, J., and Lu, J. EmbodiedSAM: Online segment any 3D thing in real time. In *Proceedings of the International Conference on Learning Representations*, 2025.
- Yadav, K., Ramrakhya, R., Ramakrishnan, S. K., Gervet, T., Turner, J., Gokaslan, A., Maestre, N., Chang, A. X., Batra, D., Savva, M., Clegg, A. W., and Chaplot, D. S. Habitat-matterport 3D semantics dataset. In *Proceedings of the IEEE/CVF Conference on Computer Vision and Pattern Recognition (CVPR)*, 2023.
- Yang, Y., Yang, H., Zhou, J., Chen, P., Zhang, H., Du, Y., and Gan, C. 3D-Mem: 3D scene memory for embodied exploration and reasoning. In *Proceedings of the IEEE/CVF Conference on Computer Vision and Pattern Recognition (CVPR)*, pp. 17294–17303, 2025.
- Yin, H., Xu, X., Wu, Z., Zhou, J., and Lu, J. SG-Nav: Online 3D scene graph prompting for LLM-based zero-shot object navigation. In *Advances in Neural Information Processing Systems*, volume 37, pp. 5285–5307, 2024.
- Yin, H., Xu, X., Zhao, L., Wang, Z., Zhou, J., and Lu, J. UniGoal: Towards universal zero-shot goal-oriented navigation. In *Proceedings of the IEEE/CVF Conference on Computer Vision and Pattern Recognition (CVPR)*, 2025.
- Yokoyama, N., Ha, S., Batra, D., Wang, J., and Bucher, B. VLFM: Vision-language frontier maps for zero-shot semantic navigation. In *Proceedings of the IEEE International Conference on Robotics and Automation (ICRA)*, pp. 42–48, 2024.
- Yu, B., Kasaei, H., and Cao, M. L3MVN: Leveraging large language models for visual target navigation. In *Proceedings of the IEEE/RSJ International Conference on Intelligent Robots and Systems (IROS)*, pp. 3554–3560, 2023.
- Zeng, S., Qi, D., Chang, X., Xiong, F., Xie, S., Wu, X., Liang, S., Xu, M., and Wei, X. JanusVLN: Decoupling semantics and spatiality with dual implicit memory for vision-language navigation. *arXiv preprint arXiv:2509.22548*, 2025.
- Zhang, J., Wang, K., Xu, R., Zhou, G., Hong, Y., Fang, X., Wu, Q., Zhang, Z., and Wang, H. NaVid: Video-based VLM plans the next step for vision-and-language navigation. *arXiv preprint arXiv:2402.15852*, 2024a.
- Zhang, L., Zhang, Q., Wang, H., Xiao, E., Jiang, Z., Chen, H., and Xu, R. TriHelper: Zero-shot object navigation with dynamic assistance. In *Proceedings of the IEEE/RSJ International Conference on Intelligent Robots and Systems (IROS)*, pp. 10035–10042, 2024b.
- Zhang, L., Hao, X., Xu, Q., Zhang, Q., Zhang, X., Wang, P., Zhang, J., Wang, Z., Zhang, S., and Xu, R. MapNav: A novel memory representation via annotated semantic maps for VLM-based vision-and-language navigation. In *Proceedings of the 63rd Annual Meeting of the Association for Computational Linguistics*, pp. 13032–13056, 2025a.
- Zhang, M., Du, Y., Wu, C., Zhou, J., Qi, Z., Ma, J., and Zhou, B. ApexNav: An adaptive exploration strategy for zero-shot object navigation with target-centric semantic fusion. *IEEE Robotics and Automation Letters*, 10(11): 11530–11537, 2025b.
- Zhang, S., Yu, X., Song, X., Wang, X., and Jiang, S. Imagine before go: Self-supervised generative map for object goal navigation. In *Proceedings of the IEEE/CVF Conference on Computer Vision and Pattern Recognition (CVPR)*, pp. 16414–16425, 2024c.
- Zhang, S., Qiao, Y., Wang, Q., Guo, L., Wei, Z., and Liu, J. FlexVLN: Flexible adaptation for diverse vision-and-language navigation tasks. *IEEE Transactions on Multimedia*, 27:6307–6318, 2025c.
- Zhang, Y., Yang, S., Bai, C., Wu, F., Li, X., Wang, Z., and Li, X. Towards efficient LLM grounding for embodied multi-agent collaboration. In *Findings of the Association for Computational Linguistics: ACL 2025*, pp. 1663–1699, 2025d.
- Zhong, L., Gao, C., Ding, Z., Liao, Y., Ma, H., Zhang, S., Zhou, X., and Liu, S. TopV-Nav: Unlocking the top-view spatial reasoning potential of MLLM for zero-shot object navigation. *arXiv preprint arXiv:2411.16425*, 2025.

Zhou, G., Hong, Y., Wang, Z., Wang, X. E., and Wu, Q. NavGPT-2: Unleashing navigational reasoning capability for large vision-language models. In *Proceedings of the European Conference on Computer Vision (ECCV)*, pp. 260–278, 2024a.

Zhou, G., Hong, Y., and Wu, Q. NavGPT: Explicit reasoning in vision-and-language navigation with large language models. In *Proceedings of the AAAI Conference on Artificial Intelligence*, volume 38, pp. 7641–7649, 2024b.

Zhou, K., Zheng, K., Pryor, C., Shen, Y., Jin, H., Getoor, L., and Wang, X. E. ESC: Exploration with soft commonsense constraints for zero-shot object navigation. In *Proceedings of the International Conference on Machine Learning*, volume 202, pp. 42829–42842, 2023.

A. DSCD-Nav Details

This appendix summarizes the key components required to reproduce our method, including the action-selection pseudocode, implementation settings, micro-probing sensitivity analysis, and experimental metrics.

A.1. DSCD-Nav Action Selection Pseudocode

We provide step-by-step pseudocode for DSCD-Nav action selection used in all experiments.

Algorithm 1 DSCD-Nav Action Selection

```

1: Input: observation  $o_t$ , goal  $g$ , candidate set  $\mathcal{A}_t$ , optional evidence  $\mathcal{E}_t$ 
2: Output: executable action  $(r_{exec}, \theta_{exec})$ 
3: Initialize  $\mathcal{C}_t \leftarrow \Phi(\mathcal{A}_t)$ , and set  $X_t \leftarrow (g, \mathcal{C}_t, \mathcal{E}_t)$ 
4: Initialize debate history  $\mathcal{H}^{(0)} \leftarrow \emptyset$ 
5:  $k \leftarrow 1$ ;  $cons \leftarrow false$ 
6: while  $(k \leq K)$  and  $(cons = false)$  do
7:   TSU proposes  $(id_{TSU}^{(k)}, w_{TSU}^{(k)}, ev_{TSU}^{(k)})$ 
8:   SIB responds with  $(dec^{(k)}, id_{SIB}^{(k)}, w_{SIB}^{(k)}, ev_{SIB}^{(k)})$ 
9:   Update  $\mathcal{H}^{(k)}$ 
10:  if  $dec^{(k)} = agree$  then
11:     $cons \leftarrow true$ 
12:  end if
13:   $k \leftarrow k + 1$ 
14: end while
15: Collect all rounds into  $\mathcal{D}_t$ 
16: NCA outputs  $(id^*, w^*, ev^*)$ 
17: Retrieve  $(r^*, \theta^*)$  from  $\mathcal{C}_t$  by  $id^*$ 
18: Let  $\theta^{alt}$  be the heading suggested by the non-selected
19:  $\Delta\theta \leftarrow \text{wrap}(\theta^{alt} - \theta^*)$ 
20: if  $|\Delta\theta| \leq \alpha$  then
21:    $(r_{exec}, \theta_{exec}) \leftarrow \text{SOFTCOMPROMISE}((r^*, \theta^*), \theta^{alt})$ 
22: else
23:    $(r_{exec}, \theta_{exec}) \leftarrow (r^*, \theta^*)$ 
24: end if
25: Log  $\mathcal{D}_t$ ,  $id^*$ , and compromise flags
26: return  $(r_{exec}, \theta_{exec})$ 

```

A.2. Experimental Setup Details

Implementation Details. The maximal navigation steps per episode are set to 40. The agent’s body has a radius of 0.17m and a height of 1.5m. Its RGB-D sensors are positioned at 1.5m height with a -0.45 radian downward tilt and provide a 131° field of view (FoV). For rotation, the agent selects an angular displacement from 60 discrete bins with a maximum interval of 0.5 radians. Success requires stopping within $d_{\text{success}} = 0.5\text{m}$ of the target object and visually confirming it. Our DSCD-Nav framework primarily utilizes Gemini-2.5-Flash-Lite through the official public API as the base vision-language model and CLIP ViT-B/32 for semantic embeddings, with caching implemented for efficiency. We set the debate rounds to `Rounds = 3`, and enable micro-probing with a maximum angular interval of $\Delta\theta_{\text{max}} = 60^\circ$, a length scaling factor of $\beta_r = \frac{1}{2}$, and an angular bias ratio of $\beta_\theta = \frac{1}{3}$. In addition, we employ GroundingDINO as evidence-prompt augmentation to strengthen stop verification and improve termination reliability.

A.3. Micro-Probing Sensitivity Analysis

We study the sensitivity of micro-probing on the HM3D ObjectNav benchmark (HM3Dv1) under a stricter episode budget, where the maximum number of navigation steps is capped at 20. We keep the entire pipeline identical to the main configuration and vary only two execution hyperparameters: β_r , which scales the forward motion, and β_θ , which controls

Table 5. Sensitivity of micro-probing hyperparameters on HM3Dv1 under a 20-step episode budget. We vary (β_r, β_θ) while keeping all other settings fixed.

Parameter	Default	Range	SR(%) \uparrow	SPL(%) \uparrow
β_r	0.50	[0.33, 0.50, 0.67]	75.6 [74.9, 75.6 , 75.2]	40.1 [39.7, 40.1 , 39.2]
β_θ	0.33	[0.25, 0.33, 0.50]	75.6 [75.3, 75.6 , 75.1]	40.1 [39.9, 40.1 , 39.6]

the yaw interpolation toward the alternative direction. The probe is triggered only when the final-round preferences remain inconsistent yet geometrically close, i.e., the directional gap falls within the threshold α ; otherwise we execute the NCA-arbitrated action (Mode A). Table 5 shows that the resulting changes in SR and SPL are mild over a reasonable range of β_r and β_θ , indicating that our gains do not hinge on a particular choice of the default coefficients.

A.4. Experimental Metrics

We report standard 3D navigation metrics, including *Success Rate* (SR) and *Success weighted by Path Length* (SPL), and further adopt *Area Overlap Redundancy Index* (AORI) to quantify redundant exploration. In addition, we introduce debate-specific metrics to characterize disagreement and arbitration behaviors, including *Round-level Disagreement Rate* (DR), *Judge Override Rate* (JOR), and *Micro-Probing Trigger Rate* (MPTR).

Success Rate (SR). SR measures the fraction of successful episodes:

$$SR = \frac{1}{N} \sum_{i=1}^N S_i, \quad (14)$$

where N is the number of episodes and $S_i \in \{0, 1\}$ indicates whether episode i succeeds (i.e., the agent stops within the success threshold and visually confirms the target).

Success weighted by Path Length(SPL). SPL balances success with path efficiency:

$$SPL = \frac{1}{N} \sum_{i=1}^N S_i \cdot \frac{l_i}{\max(p_i, l_i)}, \quad (15)$$

where l_i is the shortest-path (geodesic) distance from the start to the goal in episode i , and p_i is the agent’s traveled path length.

Area Overlap Redundancy Index (AORI). Consider an episode of length T with agent locations $\{(x_t, y_t)\}_{t=1}^T$. Let $\mathcal{V}_t = \mathcal{V}(x_t, y_t)$ denote the visible region at step t , and let $A_t = \bigcup_{i=1}^t \mathcal{V}_i$ denote the accumulated observed area up to step t , where $\|\cdot\|$ measures area or voxel count. We define the revisit overlap ratio as:

$$r_{\text{overlap}} = \frac{1}{T-1} \sum_{t=2}^T \frac{1}{t-1} \sum_{i=1}^{t-1} \mathbb{I}[\|\mathcal{V}_t \cap \mathcal{V}_i\| \geq \tau], \quad (16)$$

where τ is the overlap threshold. Intuitively, r_{overlap} measures how frequently the current visible region substantially overlaps previously observed regions.

We further define the normalized exploration density as:

$$d_{\text{norm}} = \frac{1}{T} \sum_{t=1}^T \min\left(1, \frac{N_{\text{obs}}^{(t)}}{\lambda_t}\right), \quad \lambda_t = \eta \cdot \frac{\|A_t\|}{\text{map_size}^2} \cdot t, \quad (17)$$

where $N_{\text{obs}}^{(t)}$ counts the number of voxels that have been visited at least three times up to step t , and η is a scaling factor. In our implementation, the visible region size is given by:

$$\|\mathcal{V}(x, y)\| = \frac{\text{map_size}^2}{\text{voxel_ray_size}^2} \pi. \quad (18)$$

Finally, AORI combines the two terms to quantify redundancy:

$$\text{AORI} = 1 - \left(w_c (1 - r_{\text{overlap}})^2 + w_d (1 - d_{\text{norm}}) \right), \quad (19)$$

where $w_c = 0.8$ and $w_d = 0.2$. Lower AORI indicates less redundant exploration.

Round-level Disagreement Rate (DR). DR measures how often TSU and SIB prefer different candidate actions across all debate rounds. For step i , let R_i be the number of debate rounds, and let $a_{i,r}^{\text{TSU}}$ and $a_{i,r}^{\text{SIB}}$ denote the preferred candidate id at round r . Then:

$$\text{DR} = \frac{\sum_{i=1}^N \sum_{r=1}^{R_i} \mathbb{I}[a_{i,r}^{\text{TSU}} \neq a_{i,r}^{\text{SIB}}]}{\sum_{i=1}^N R_i}, \quad (20)$$

where $\mathbb{I}[\cdot]$ is the indicator function.

Judge Override Rate (JOR). JOR is computed only on steps that enter arbitration at the final round. Let R_{max} be the maximal rounds (e.g., 3) and define the arbitration set:

$$\mathcal{A} = \{i \mid R_i = R_{\text{max}}, a_{i,R_{\text{max}}}^{\text{TSU}} \neq a_{i,R_{\text{max}}}^{\text{SIB}}, a_i^J \text{ exists}\}, \quad (21)$$

where a_i^J is the final decision produced by the judge. JOR measures the fraction of cases where the judge does not adopt TSU’s final preference:

$$\text{JOR} = \frac{\sum_{i \in \mathcal{A}} \mathbb{I}[a_i^J \neq a_{i,R_{\text{max}}}^{\text{TSU}}]}{|\mathcal{A}|}. \quad (22)$$

Micro-Probing Trigger Rate (MPTR). MPTR is also computed on \mathcal{A} and measures how often the execution switches to micro-probing mode during arbitration. Let $c_i \in \{0, 1\}$ indicate whether micro-probing is triggered at step i , then:

$$\text{MPTR} = \frac{\sum_{i \in \mathcal{A}} c_i}{|\mathcal{A}|}. \quad (23)$$

B. Supplementary Examples

This appendix provides supplementary quantitative results and qualitative case studies, including a comparison with training-free VLM-based baselines, representative navigation episodes with step-level debate traces and top-down trajectories, and a detailed description of the evaluated baselines.

B.1. Quantitative Comparison

Training-free VLM-based baselines. Table 6 provides an additional comparison between our method and representative training-free VLM-based navigation baselines. All methods follow a prompt-driven decision pipeline under the same evaluation protocol, and we report SR and SPL for reference. The results highlight that DSCD achieves stronger task success and path efficiency than prior VLM-centric approaches in this setting.

Table 6. Comparison with training-free VLM-based navigation baselines on HM3D ObjectNav.

Method	SR (%)↑	SPL (%)↑
Prompt-only	29.8	10.7
PIVOT	24.6	10.6
VLMNav	51.6	18.3
NavGPT-2	47.2	28.0
WMNav	58.1	31.2
DORAEMON	62.0	23.0
DSCD (Ours)	75.6	40.1

B.2. Qualitative Examples

Navigation Case and Debate Trace. Figure 6 shows a navigation case and debate trace for the goal *bed* at an ambiguous junction. Instead of committing via one-shot scoring, the two stances cross-check the scene: TSU prioritizes goal progress, while SIB audits risk and visibility to keep options open under partial observability. The NCA judge then arbitrates based on the most salient local cues, selecting a balanced action that preserves observability while still advancing the search. Overall, the debate–arbitration loop reduces premature commitment and redundant backtracking, yielding a controlled, evidence-grounded decision, as also reflected by the top-down trajectory view in Fig. 5.



Figure 5. Top-down trajectory visualization. The floor-plan view overlays the agent’s navigation trace within the scene. Colored arrows denote the executed motions and a small set of salient alternative directions at key junctions, while red crosses mark branches that are discarded or lead to failures or inefficient detours.

B.3. Detailed Description of Baselines

To assess the performance of DSCD, we compare against a broad set of representative ObjectNav baselines on HM3D and MP3D, spanning learning-based map and exploration pipelines and recent foundation-model–driven micro-probing (or soft-compromise) zero-shot planners.

- **SemExp**: Goal-oriented semantic exploration that builds an online semantic map and plans search using semantic cues.
- **ProcTHOR**: Procedurally generated large-scale indoor scenes widely used for scalable embodied navigation training.
- **ZSON**: Zero-shot ObjectNav baseline leveraging vision-language goal embeddings to generalize to unseen categories.

- **PONI**: Interaction-free learning of potential functions over semantic maps to guide object-goal navigation.
- **PSL**: Prioritized semantic learning that improves zero-shot transfer with semantics-aware inference.
- **Habitat-Web**: Web-collected human demonstrations used to train object-search behavior via imitation.
- **ProcTHOR-ZS**: Zero-shot cross-domain evaluation where ProcTHOR-trained models are tested in unseen environments.
- **Pixel-Nav**: Pixel-conditioned navigation that uses visual goal specification to guide long-horizon action selection.
- **SGM**: Self-supervised generative mapping that predicts unobserved regions to boost exploration efficiency.
- **VLFM**: Frontier-based exploration guided by vision-language grounding to score and select promising frontiers.
- **CoW**: Training-free CLIP-based baseline family combining goal localization with exploration for language-driven zero-shot ObjectNav.
- **ESC**: Soft commonsense constraints injected into zero-shot exploration to reduce implausible and inefficient search.
- **L3MVN**: LLM commonsense priors used to propose long-term goals, with a visual policy executing the suggested path.
- **TriHelper**: Helper-augmented navigation that improves stability under common failure modes in object search.
- **OpenFMNav**: Open-vocabulary navigation using foundation perception to build semantic score maps for decision making.
- **InstructNav**: Training-free instruction navigation using chain-style decision making with multi-source value estimation.
- **SG-Nav**: Online 3D scene graph construction with structured hierarchical prompting for explainable reasoning.
- **OneMap**: Training-free CLIP-based mapping baseline that maintains an online open-vocabulary belief map to localize text goals and guide exploration for zero-shot ObjectNav.
- **TopV-Nav**: MLLM reasoning on top-view map representations with adaptive prompting and dynamic map scaling.
- **CogNav**: Cognitive-state navigation that performs stateful reasoning over structured memory and belief updates.

round1: TSU: id 4.

why: it steers toward the living-area branch that likely connects to bedrooms
evidence: A living room with a couch is visible ahead-right. The current view is a dining/kitchen boundary, typically not where beds are located.



SIB: counter, id 2.

why: Action 4 may be an overly aggressive rightward commitment. Action 2 provides a milder turn that preserves visibility.
evidence: Smaller yaw keeps both paths in view; improves safety and information gain under layout uncertainty; avoids prematurely locking into a single branch.

round3: TSU: id 2.

why: Your point on controlled rightward exploration is valid. Action 2 aligns with the visible right-side transition.
evidence: Action 2 is a balanced step toward the living-room-connected area while maintaining a stable approach for potential bedroom discovery.



GOAL:BED STEP 0



NCA: prefer id 2.

why: id 2 is the most justified compromise between task-driven pursuit of the right-side branch and safety/information-aware conservatism.
evidence: Right-side opening is the strongest cue to private rooms. A moderate yaw preserves visibility and reduces over-commitment risk.



round1: TSU: id 1.

why: Forward-left targets the nearest left-side doors, which are the most immediate candidates for bedroom entries in a typical hallway layout.
evidence: Hallways commonly have bedrooms along the sides. The living area visible ahead is not a bedroom, so doors are the primary focus.



SIB: counter, id 2.

why: Action 1 is a sharp leftward commitment that may prematurely narrow the field of view, reducing visibility of other doors and the staircase. Action 2 provides a more moderate leftward shift while preserving a broader view of the hallway for better information gain.
evidence: A smaller yaw keeps both left and right door rows in sight. Under layout uncertainty, a balanced approach improves safety and exploration efficiency.

round3: TSU: agree, id 2.

why: A moderate left turn still approaches the left doors while retaining the flexibility to observe other areas, aligning better with the need for cautious exploration when no bed is yet visible.
evidence: A less aggressive turn reduces the risk of missing alternative paths. The task goal requires efficient search, but early over-commitment could lead to dead ends.



GOAL:BED STEP 1



NCA: prefer id 2.

why: A moderate leftward move best balances task-driven exploration of the left-side doors with the safety and information-gain benefits.
evidence: The visual analysis reports no bed visible yet, emphasizing the need for cautious, informative exploration. Preserving visibility minimizes the chance of overlooking a bedroom entrance.



round1: TSU: id 1.

why: Forward-left aligns with the left-side doors, the most probable entries to a bedroom based on household layout priors.

evidence: Left-side doors in a hallway commonly lead to bedrooms.

Action 1 provides focused progression toward the most promising branch.



SIB: counter, id 2.

why: Action 1 may pose collision risk and reduces visibility ahead in a narrow hallway. Action 2 maintains forward progression while preserving broader frontal view of both door rows.

evidence: Action 2 keeps both left and right doors in view for ongoing assessment; allows for later flexible turns based on door-state clues.

round3: TSU: id 1.

why: The deeper left door may be a bedroom; delaying approach could extend search time.

evidence: Memory context notes bedrooms are typically along hallways. Action 1 still permits subsequent rightward adjustment if needed.



SIB: agree, id 1.

why: After reassessment, the left-door exploration priority aligns with both task progression and manageable risk.

evidence: The corridor is clearly laid out, facilitating the observation of post-steps. A subsequent rotation can address any visibility shortfall.

GOAL:BED STEP 2



NCA: prefer id 1.

why: Both stances converge on id 1 after debate, indicating that left-door exploration balances task progress and acceptable risk.

evidence: Left-side doors are top candidates for bedroom location. Consensus allows direct execution without geometric compromise.



round1: TSU: id 2.

why: Bed is clearly visible through the right doorway. Forward-right is the most direct action to approach it.

evidence: bed is visible through an open doorway to the right.



SIB: agree, id 2.

why: Moving directly toward the visible bed now offers a good balance of progress and acceptable risk.

evidence: No immediate obstacles or collision risks detected. High-confidence target visibility reduces the need for exploratory caution.

GOAL:BED STEP 3



NCA: prefer id 2.

why: Direct approach toward the visually confirmed bed is both task-optimal and safe under the clear current evidence.

evidence: Both stances agree on id 2 without requiring counter-debate. Visual evidence strongly supports a clear, unobstructed path.





Figure 6. Navigation case and debate trace. Each row corresponds to one decision step along the trajectory, with the executed action highlighted in green. The debate trace summarizes TSU’s goal-progress proposal, SIB’s safety and visibility audit, and the NCA judge’s final arbitration grounded in the current scene evidence.